Featured in Physics

Vibrational Modes and Particle Rearrangements in Sheared Quasi-Two-Dimensional Complex Plasmas

Yang Miao, ^{1,†} Alexei V. Ivlev, ² Hartmut Löwen, ³ Volodymyr Nosenko, ⁴ He Huang, ¹ Wei Yang, ^{1,5}

Hubertus M. Thomas, ⁴ Jing Zhang, ^{1,5} and Cheng-Ran Du, ^{1,5,*}

College of Physics, Donghua University, 201620 Shanghai, People's Republic of China

Max-Planck-Institut für Extraterrestrische Physik, 85748 Garching, Germany

Institut für Theoretische Physik II: Weiche Materie, Heinrich-Heine-Universität Düsseldorf, 40225 Düsseldorf, Germany

Institut für Materialphysik im Weltraum, Deutsches Zentrum für Luft- und Raumfahrt (DLR), 51170 Cologne, Germany

Member of Magnetic Confinement Fusion Research Centre, Ministry of Education, 201620 Shanghai, People's Republic of China

(Received 26 May 2024; revised 27 June 2025; accepted 5 August 2025; published 24 September 2025)

In dense colloids and simulated glasses, it has been discovered that plastic particle rearrangements correlate with nonphononic low-frequency vibrational modes. Here, we demonstrate that this correlation also holds for a very different material class of complex plasmas under shear, characterized by long-range interactions and nonreciprocal forces. We perform experiments with a deformed amorphous quasi-two-dimensional binary complex plasma under optical pressure, which gives rise to a controlled shear rate, and confirm our findings with extensive particle-resolved computer simulations.

DOI: 10.1103/6bjy-m2j4

A central question in condensed matter physics is how to predict when and under what conditions materials break under externally imposed mechanical shear. This is of fundamental importance for applications ranging from the prediction of earthquakes [1,2] to shear melting of colloidal solids [3–5]. While crystals accumulate defects under shear that may proliferate significant plastic events and final cracking [6,7], the situation is less clear for amorphous solids. Recent studies for colloidal suspensions [8–11] and sheared granules [12-15] have revealed that plastic transformation zones largely correlate with nonphononic low-frequency vibrational modes [16–19]. This important finding allows one to identify critical spots in the amorphous solid on the particle scale where plastic events could most easily be nucleated. Still up to now this intriguing criterion has been verified experimentally only for colloid suspensions [20,21] and in various molecular model glasses explored by computer simulations [22,23].

In this Letter, we demonstrate that the correlation between plastic events and nonphononic vibrations is much more general: it also holds for a very different material class of complex plasmas [24–27]. Complex plasmas are composed of weakly ionized gases and micron-sized charged particles. As the background gas is dilute, the particle dynamics is virtually undamped and generic phenomena in regular crystals, glasses, and liquids can be studied on the kinetic

level [28–33]. As opposed to colloids and granulates where the interactions are typically short-ranged, complex plasmas exhibit long-ranged screened Coulomb interactions between the particles [34–36]. More importantly, these interaction forces are nonreciprocal, i.e., they violate Newton's third law [37–40], and are therefore representative of an entirely new material class of active matter, which is intrinsically in nonequilibrium on the particle scale.

These features of complex plasmas have significant impacts. First of all, it could be expected that the longranged interactions present in these strongly coupled systems have a significant influence on the low-frequency vibrations. Strongly coupled Coulomb systems are hyperuniform [41] and hyperuniformity suppresses any structural correlations at zero wave number. One could therefore conjecture that these long-ranged interactions will drastically affect lowfrequency phonons, and could therefore destroy the correlation with particle rearrangements. Second, nonreciprocal interactions can give rise to activity and can generate selfpropelled particle pairs [42]. For such active systems, it is known that the vibrational modes possess not only phonons but they exhibit additional new modes that are responsible for entropy production in these non-Hamiltonian systems. The latter nonphononic modes are called "entropons" [43,44]. Whether these new modes affect the correlation between plastic events and low-frequency modes is therefore a priori not clear and needs to be explored. Here, we perform experiments with a deformed amorphous quasi-twodimensional binary complex plasma under optical pressure, which gives rise to a controlled shear rate, and confirm our findings with extensive particle-resolved computer simulations involving nonreciprocal forces.

^{*}Contact author: chengran.du@dhu.edu.cn

[†]Present address: School of Physics and Astronomy, Institute of Natural Sciences, Shanghai Jiao Tong University, Shanghai 200240, People's Republic of China.

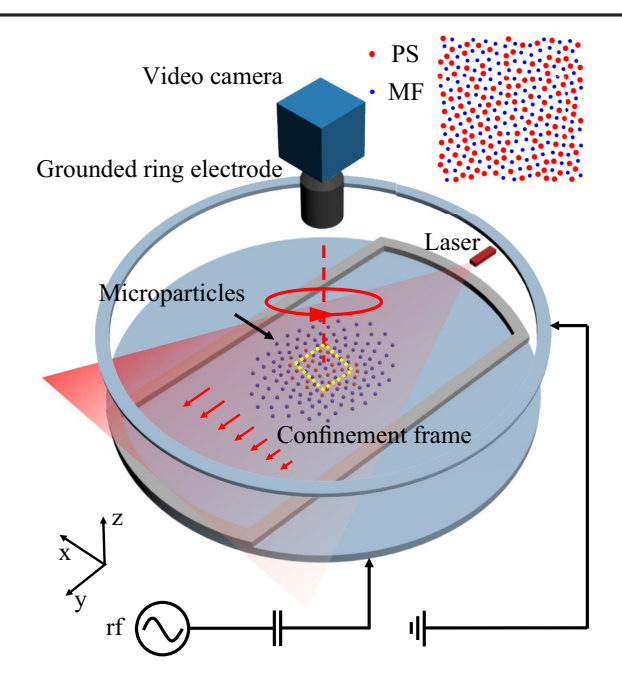


FIG. 1. Setup of the experiments. Micron-sized particles are suspended above the bottom electrode in a capacitively coupled rf discharge and confined in an aluminum frame, resulting in an elliptical configuration. Melamine formaldehyde (MF) and polystyrene (PS) particles (colored in blue and red) are mixed in the center of the particle suspension and form a disordered quasi-two-dimensional amorphous solid, as shown in the inset. Note that the interaction between MF and PS particles is nonreciprocal due to the presence of ion wake in the sheath. Driven by the inhomogeneity of the illumination laser intensity, depicted by the red arrows, the particle suspension slowly rotates.

The experiment has been conducted in a modified Gaseous Electronics Conference reference cell at a gas pressure of 5 mTorr, as shown in Fig. 1. Melamine formaldehyde and polystyrene particles with diameters of $\phi_s = 9.19 \ \mu m$ and $\phi_b = 11.36 \ \mu m$ are dispensed into the capacitively coupled radio-frequency discharge in argon [45–48]. Their masses are $m_s = 6.1 \times 10^{-13}$ kg and $m_b = 8.0 \times 10^{-13}$ kg, respectively. The particles are heavily charged via interaction with ions and electrons in the plasma and the charge value is proportional to the particle diameter [49]. In the experiment, we selected the material and size of these two types of particles such that they can be suspended by the electric field at a similar height in the sheath. As the discharge power increases from 1 to 20 W within a few seconds, the particles are instantaneously confined into a layer, where an amorphous binary mixture is formed in the center surrounded by the crystal composed of melamine formaldehyde particles, as shown in Fig. 1. The horizontal interparticle distance is $\Delta \sim 600 \mu m$, roughly 4 times as much as the vertical distance between two particle types. The existence of this small vertical distance results in the nonreciprocity of the interaction due to the ion wake effect in the plasma sheath. As there do not exist vertical pairs in the particle

suspension, it can be reasonably regarded as a quasi-twodimensional system.

For the experimental diagnostics, a horizontal laser sheet with a small width illuminates the particles from the side and particle positions are recorded as bright spots by a top-view video camera equipped with a corresponding bandpass filter at a frame rate of 60 frames/s. The recorded video sequences are further analyzed and the trajectories of individual particles are obtained. The illumination laser sheet is slightly tilted, and the weak inhomogeneity of the optical pressure provides a small torque, driving the particle suspension to rotate slowly [50,51]. We have placed an aluminum frame on the electrode so that the particle suspension is compressed in one direction by the sheath field [30]. The circular particle suspension in the cylindrical discharge cell is deformed and has an elliptical shape, as shown in Fig 1. The distance between two parallel sides of the frame can be controlled by placing different frames. As a result, a narrower confinement frame results in a bigger aspect ratio a/b of the two elliptical axes of the particle suspension, leading to the decrease of the angular velocity Ω of the rotation. This eventually increases the global shear rate, which can be estimated as $\dot{\gamma} = (4/\pi)[1 - (b/a)]\Omega$ [see Supplemental Material (SM) [52] for details].

To supplement the experimental investigation, we have performed Langevin dynamics simulations under a similar setup, considering the nonreciprocal interparticle interaction [58,59]. The simulations are conducted with the LAMMPS Molecular Dynamics Simulator [60]. In total 8100 particles are confined within a bilayer in the z direction, similar to the experiment. The ion wake effect in the plasma sheath is considered by applying a point wake model, where the vertical distance between the pointlike wake charge and the particle is set as $\delta = 90 \, \mu m$. Further information on the interactions can be found in SM [52]. The charges of the small and big particles are set as $Q_s =$ $13\,000e$ and $Q_b = 16\,000e$, respectively, and the corresponding wake charge ratio is assumed as q/Q = 0.6. The Debye length is $\lambda_D = 400 \ \mu m$. The total interaction is then composed of the reciprocal part from the direct interparticle repulsion and the nonreciprocal part from the particle-wake attraction [37]. In the xy plane, the particles are confined by the parabolic potential, where the prefactor in the x component is larger than that in the y component. As a result, the particle suspension has an elliptical shape as in the experiment. The inhomogeneous optical pressure from the illumination laser is simulated by an external force in the y direction with a gradient along the x axis. The gradient of the external force can be adjusted such that the angular velocity of the rotating particle suspension is controlled.

Despite the presence of the nonreciprocal interaction between the particles of different types, the mode coupling instability is suppressed by the electric field in the sheath in our experiment [61]. The particle suspension is stable throughout the measurement with a steady temperature.

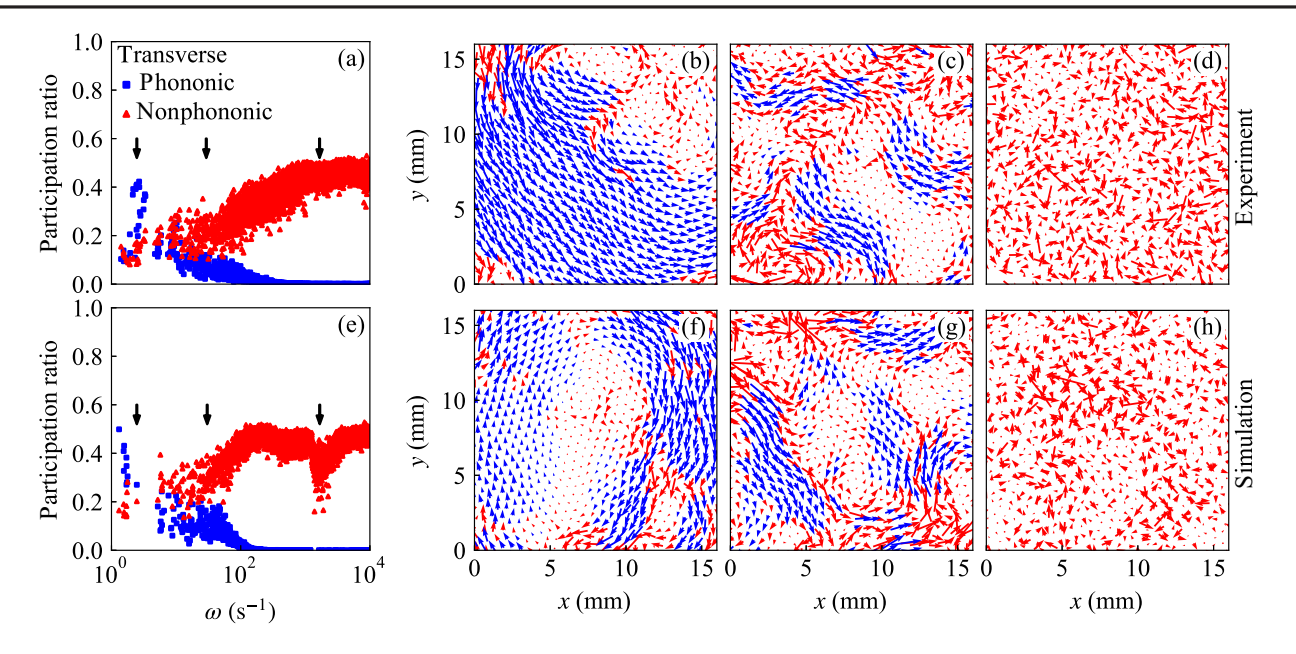


FIG. 2. Participation ratio and eigenvector fields of the transverse modes in the experiment (a)–(d) and simulation (e)–(h) for the shear rate $\dot{\gamma} \approx 2.7 \times 10^{-4} \text{ s}^{-1}$. The eigenvector fields for the low [(b), (f)], middle [(c), (g)], and high [(d), (h)] frequencies are shown for the phononic (blue) and nonphononic (red) modes in the selected region of interest, where the corresponding frequencies are indicated by the arrows in the panels (a), (b). Note that the swirl in panels (b), (f) may relate to the rotation of the particle suspension.

As a result, linear response theory can be applied to our system to describe the dynamical behaviors including wave modes [46,62,63], etc. Here, we analyze the vibrational modes based on the displacement correlation matrix $C_{mn} = \langle u_m(t)u_n(t)\rangle$, where m and n are the subscripts of the matrix, $u_{2i} = x_i(t) - \langle x_i \rangle$ and $u_{2i+1} = y_i(t) - \langle y_i \rangle$ are the displacements of the particle i from its average position in the x and y component, respectively [64-66]. The corresponding eigenvalues λ can be obtained by diagonalizing C_{mn} and thus the eigenfrequency reads $\omega =$ $\sqrt{U_0/\bar{m}\lambda}$, where $U_0 = Q_sQ_b/4\pi\epsilon_0\Delta$ and $\bar{m} = (m_s + 1)$ m_b)/2. These modes are decomposed into longitudinal and transverse parts at each frequency, using a divergence operator based on the Voronoi volume matrix method [67]. As indicated by the density of states, the transverse part plays a more important role than the longitudinal part in the low-frequency regime (see SM [52]). In the rest of this Letter, we focus on the transverse part and decompose it into phononic and nonphononic components by calculating the spatial coherence ψ_i of eigenvectors \mathbf{e}_{λ} [68],

$$\psi_i = \frac{1}{n_i} \sum_{j}^{n_i} \frac{\mathbf{e}_{\lambda}^i \cdot \mathbf{e}_{\lambda}^j}{|\mathbf{e}_{\lambda}^i| |\mathbf{e}_{\lambda}^j|},\tag{1}$$

where n_i is the number of nearest neighboring particles j of the particle i. The eigenvectors are defined as phononic modes if $\psi_i > 0.95$. The degree of localization of a vibrational mode can be quantified by the participation ratio [69–73]

$$R_p = \frac{\left(\sum_i^N |\mathbf{e}_{\lambda}^i|^2\right)^2}{N\sum_i^N |\mathbf{e}_{\lambda}^i|^4},\tag{2}$$

where N is the total number of the particles in the region of interest containing binary mixture. Every particle participates equally in the mode for $R_p=1$, whereas only a single particle participates in the mode for $R_p=1/N$. Figures 2(a) and 2(e) show the participation ratio in the experiment and simulation, respectively. The overall angular velocity is $\Omega \simeq 0.43 \times 10^{-3}$ rad/s and the geometric ratio of the elliptical particle suspension is $a/b \simeq 1.75$. It can be seen that phononic modes attenuate rapidly with frequency, which is caused by the loss of the propagating phonons. On the contrary, the nonphononic modes increase because of the strong scattering of the phonons.

The spatial distribution of eigenvectors can be used to characterize the vibrational modes of the corresponding frequencies. The typical transverse modes of three frequency regimes in the experiment and simulation are depicted in Figs. 2(b)–2(d) and 2(f)–2(h), respectively. Here, blue arrows represent the phononic modes and red arrows represent the nonphononic modes. For the low-frequency modes, the phononic component dominates and both the directions and amplitudes of the eigenvectors are highly coherent in space. As the frequency gradually increases, vortexlike structures are observed for phononic component. For the high-frequency regime, the phononic modes vanish and the nonphononic modes become disordered such that their directions and amplitudes are strongly randomized.

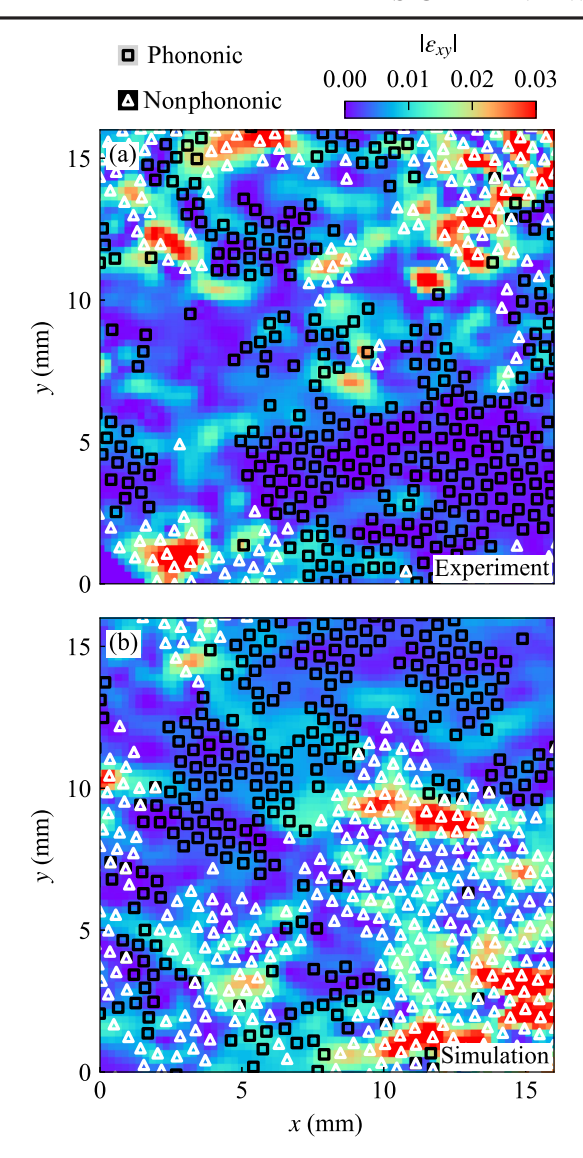


FIG. 3. Correlation between the local shear strain and the strength of transverse modes of low frequencies in the experiment (a) and simulation (b) in the selected region of interest. The particle positions with summed amplitudes exceeding a threshold of 0.12 for phononic and nonphononic modes are overlaid on the contour plot of the shear strain as black squares and white triangles, respectively.

As the elliptical particle suspension slowly rotates, the anisotropic confinement shears the system, leading to the structural rearrangements [74,75]. Such particle rearrangements can be quantified by the time-dependent strain ε_{xy} , determined by minimizing the mean-squared difference between the actual displacements of the neighboring particle relative to the central one and the relative displacements that they would have if they were in a region of uniform strain [76]. The minimal difference, notated as $D_{\min}^2(\Delta t)$, is the local deviation from affine deformation for a lag time of Δt . In our experiment, we have probed the structural rearrangement by measuring the absolute shear strain distribution for a

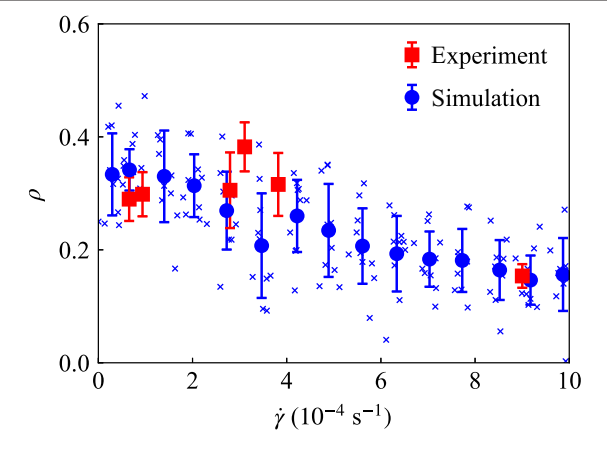


FIG. 4. Dependence of the Spearman rank correlation between the local shear strain and the strength of transverse modes of low frequencies on shear rate in experiment and simulation. Red squares are experimental results with standard deviations, resulting from the selection of different measurement areas. Blue crosses represent individual simulation runs and circles are the average correlations for each shear rate with standard deviations, resulting from the setting of different initial configurations.

time interval $\Delta t = 3.3$ s and averaged the result over 66 s. The results are shown in Fig. 3(a). The reddish areas represent the locations of high strain, while the blueish area represents the locations of low strain.

In order to investigate the connection between the irreversible particle rearrangements and the phonon dynamics at low frequency, we have summed up the amplitudes of the eigenvectors over 10 lowest modes for each particle in the experiment. The particle positions with the summed amplitude exceeding a threshold of 0.12 for the phononic and nonphononic modes are overlaid on the spatial distribution of the shear strain as black squares and white triangles, respectively, in the same experimental run in Fig. 3(a). As a result, the localized low-frequency nonphononic modes in the quasi-two-dimensional amorphous complex plasma are spatially correlated to the structural rearrangement, while the phononic modes are negatively correlated with the rearrangement. Similar results are also observed in the numerical simulation, as shown in Fig. 3(b). Thus, such correlations are a generic feature for both reciprocal (see SM [52]) and nonreciprocal interactions.

Furthermore, we investigate the correlation between the vibrational modes and rearrangement area under different shear rates in the experiment and simulation. In the experiment, we adjusted the width of the confinement such that the shape and angular velocity of the particle suspension varied. Corresponding simulations have been performed by adjusting the angular velocity of the particle suspension. The Spearman rank correlation ρ between the transverse modes and localized rearrangement areas is calculated [77–79] (see also SM for details [52]). As shown in Fig. 4, the positive correlation between the nonphononic modes and irreversible rearrangements

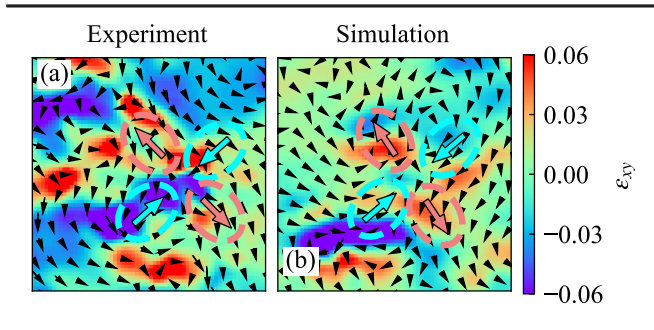


FIG. 5. Eshelby-like quadrupolar structure in the experiment (a) and simulation (b). The particle displacements within 16.6 s are overlaid on the contour plot of the shear strain as black arrows. Eshelby-like quadrupolar structures are highlighted by cyan and pink dashed ellipses.

decreases with the shear rate. Similarly, the negative correlation between the phononic modes and irreversible rearrangements also decreases. As the shear rate drastically increases, plastic events start to emerge all over the particle suspension and they begin to interact with each other. Such rearrangements are dominantly triggered by the external shear, and thus their correlation to the vibration becomes overwhelmed. This significantly reduces the Spearman correlation measured in the experiment and simulation.

It is well known that Eshelby-like quadrupolar singularities are generally correlated to the plastic events in amorphous solids [80–83]. In our experiments, we observe such quadrupolar structure in the region with relatively high shear strain, as shown in Fig. 5. There is a signature of anisotropic strain decay away from the particle rearrangements. However, due to the limit of experimental resolution, the collective effects cannot be investigated in detail.

To summarize, by a combination of experiment and simulation, we provide evidence of correlations between low-frequency nonphononic modes and structural rearrangements for a vastly different system than previously considered, namely a sheared complex plasma governed by nonreciprocal long-ranged interactions. The observed correlations decrease for increasing the imposed shear rate. Our result suggests that these correlations, which are of prime importance when it comes to predict plastic deformations in an amorphous solid, are much more general than even anticipated before. Since there is a constant energy input by the ion flux, complex plasmas belong to the class of active matter. One can therefore expect and speculate that the correlations found do also occur in other nonreciprocal interactions that induce activity such as motile tissues composed of living cells [84], dense biofilms [85], bacterial colonies [86,87], and even human crowds [88,89].

Acknowledgments—The work is supported by the National Natural Science Foundation of China (Grants

No. 12035003 and No. 11975073) and the Fundamental Research Funds for the Central Universities (Grant No. 2232023A-09). We thank T. Voigtmann for the valuable comments.

- [1] P. D. Ispńovity, D. Ugi, G. Péterffy, M. Knapek, S. Kalácska, D. Tüzes, Z. Dankházi, K. Máthis, F. Chmelík, and I. Groma, Nat. Commun. 13, 1975 (2022).
- [2] P. Kumar, R. Benzi, J. Trampert, and F. Toschi, Phys. Rev. Res. 5, 033211 (2023).
- [3] M. J. Stevens, M. O. Robbins, and J. F. Belak, Phys. Rev. Lett. 66, 3004 (1991).
- [4] C. Eisenmann, C. Kim, J. Mattsson, and D. A. Weitz, Phys. Rev. Lett. 104, 035502 (2010).
- [5] E. Yang and R. A. Riggleman, Phys. Rev. Lett. 128, 097801 (2022).
- [6] Q. An and W. A. Goddard, Phys. Rev. Lett. 115, 105501 (2015).
- [7] X. Hu, N. Liu, V. Jambur, S. Attarian, R. Su, H. Zhang, J. Xi, H. Luo, J. Perepezko, and I. Szlufarska, Nat. Mater. 22, 1071 (2023).
- [8] E. R. Weeks, J. C. Crocker, A. C. Levitt, A. Schofield, and D. A. Weitz, Science 287, 627 (2000).
- [9] J. Mattsson, H. M. Wyss, A. Fernandez-Nieves, K. Miyazaki, Z. Hu, D. R. Reichman, and D. A. Weitz, Nature (London) 462, 83 (2009).
- [10] D. Kaya, N. L. Green, C. E. Maloney, and M. F. Islam, Science 329, 656 (2010).
- [11] V. Chikkadi, G. Wegdam, D. Bonn, B. Nienhuis, and P. Schall, Phys. Rev. Lett. 107, 198303 (2011).
- [12] A. Amon, V. B. Nguyen, A. Bruand, J. Crassous, and E. Clément, Phys. Rev. Lett. 108, 135502 (2012).
- [13] A. Le Bouil, A. Amon, S. McNamara, and J. Crassous, Phys. Rev. Lett. 112, 246001 (2014).
- [14] H. Tong, H. Hu, P. Tan, N. Xu, and H. Tanaka, Phys. Rev. Lett. 122, 215502 (2019).
- [15] J. D. Sartor and E. I. Corwin, Phys. Rev. Lett. 129, 188001 (2022).
- [16] L. Wang, A. Ninarello, P. Guan, L. Berthier, G. Szamel, and E. Flenner, Nat. Commun. 10, 26 (2019).
- [17] G. Kapteijns, D. Richard, and E. Lerner, Phys. Rev. E 101, 032130 (2020).
- [18] S. Bonfanti, R. Guerra, C. Mondal, I. Procaccia, and S. Zapperi, Phys. Rev. Lett. 125, 085501 (2020).
- [19] D. Xu, S. Zhang, H. Tong, L. Wang, and N. Xu, Nat. Commun. 15, 1424 (2024).
- [20] K. Chen, M. L. Manning, P. J. Yunker, W. G. Ellenbroek, Z. Zhang, A. J. Liu, and A. G. Yodh, Phys. Rev. Lett. 107, 108301 (2011).
- [21] A. Ghosh, V. Chikkadi, P. Schall, and D. Bonn, Phys. Rev. Lett. 107, 188303 (2011).
- [22] A. Widmer-Cooper, H. Perry, P. Harrowell, and D. Reichman, Nat. Phys. 4, 711 (2009).
- [23] D. Richard, G. Kapteijns, J. A. Giannini, M. L. Manning, and E. Lerner, Phys. Rev. Lett. **126**, 015501 (2021).
- [24] R. L. Merlino and J. A. Goree, Phys. Today 57, No. 32, 7 (2004).
- [25] V. Fortov, A. Ivlev, S. Khrapak, A. Khrapak, and G. Morfill, Phys. Rep. 421, 1 (2005).

- [26] G. E. Morfill and A. V. Ivlev, Rev. Mod. Phys. 81, 1353 (2009).
- [27] A. Melzer *et al.*, *Physics of Dusty Plasmas* (Springer, New York, 2019), Vol. 962.
- [28] L. I, W.-T. Juan, C.-H. Chiang, and J. H. Chu, Science 272, 1626 (1996).
- [29] H. M. Thomas and G. E. Morfill, Nature (London) 379, 806 (1996).
- [30] C.-R. Du, V. Nosenko, H. M. Thomas, Y.-F. Lin, G. E. Morfill, and A. V. Ivlev, Phys. Rev. Lett. 123, 185002 (2019).
- [31] S. Singh, P. Bandyopadhyay, K. Kumar, and A. Sen, Phys. Rev. Lett. 129, 115003 (2022).
- [32] Y.-Y. Tsai, J.-Y. Tsai, and L. I, Nat. Phys. 12, 573 (2016).
- [33] C.-S. Wong, J. Goree, Z. Haralson, and B. Liu, Nat. Phys. 14, 21 (2017).
- [34] A. Ivlev, H. Löwen, G. Morfill, and C. P. Royall, *Complex Plasmas and Colloidal Dispersions: Particle-Resolved Studies of Classical Liquids and Solids*, (World Scientific, Singapore, 2012).
- [35] M. Chaudhuri, A. V. Ivlev, S. A. Khrapak, H. M. Thomas, and G. E. Morfill, Soft Matter 7, 1287 (2011).
- [36] S. Khrapak, Phys. Rep. 1050, 1 (2024).
- [37] A. V. Ivlev, J. Bartnick, M. Heinen, C.-R. Du, V. Nosenko, and H. Löwen, Phys. Rev. X 5, 011035 (2015).
- [38] C. Scheibner, A. Souslov, D. Banerjee, P. Surówka, W. T. M. Irvine, and V. Vitelli, Nat. Phys. 16, 475 (2020).
- [39] M. Fruchart, R. Hanai, P.B. Littlewood, and V. Vitelli, Nature (London) 592, 363 (2021).
- [40] A. Poncet and D. Bartolo, Phys. Rev. Lett. 128, 048002 (2022).
- [41] S. Torquato, Phys. Rep. 745, 1 (2018).
- [42] J. Bartnick, A. Kaiser, H. Löwen, and A. V. Ivlev, J. Chem. Phys. 144 (2016).
- [43] L. Caprini, U. Marini Bettolo Marconi, and H. Löwen, Phys. Rev. E 108, 044603 (2023).
- [44] L. Caprini, H. Löwen, and R. M. Geilhufe, Nat. Commun. 15, 94 (2024).
- [45] B. Smith, T. Hyde, L. Matthews, J. Reay, M. Cook, and J. Schmoke, Adv. Space Res. 41, 1510 (2008).
- [46] P. Hartmann, Z. Donkó, G. J. Kalman, S. Kyrkos, K. I. Golden, and M. Rosenberg, Phys. Rev. Lett. 103, 245002 (2009).
- [47] G. J. Kalman, P. Hartmann, Z. Donkó, K. I. Golden, and S. Kyrkos, Phys. Rev. E 87, 043103 (2013).
- [48] F. Wieben, J. Schablinski, and D. Block, Phys. Plasmas **24**, 033707 (2017).
- [49] J. E. Allen, Phys. Scr. 45, 497 (1992).
- [50] J. Carstensen, F. Greiner, L.-J. Hou, H. Maurer, and A. Piel, Phys. Plasmas 16, 013702 (2009).
- [51] U. Konopka, D. Samsonov, A. V. Ivlev, J. Goree, V. Steinberg, and G. E. Morfill, Phys. Rev. E 61, 1890 (2000).
- [52] See Supplemental Material at http://link.aps.org/supplemental/10.1103/6bjy-m2j4 for the supporting information of the experiments and simulations, which includes Refs. [53–57].
- [53] D. Samsonov, J. Goree, Z. W. Ma, A. Bhattacharjee, H. M. Thomas, and G. E. Morfill, Phys. Rev. Lett. 83, 3649 (1999).

- [54] M. Jambor, V. Nosenko, S. K. Zhdanov, and H. M. Thomas, Rev. Sci. Instrum. 87 (2016).
- [55] L. Couëdel, V. Nosenko, S. K. Zhdanov, A. V. Ivlev, H. M. Thomas, and G. E. Morfill, Phys. Rev. Lett. 103, 215001 (2009).
- [56] A. Melzer, V. A. Schweigert, and A. Piel, Phys. Rev. Lett. 83, 3194 (1999).
- [57] S. Plimpton, J. Comput. Phys. 117, 1 (1995).
- [58] Y.-F. Lin, A. Ivlev, H. Löwen, L. Hong, and C.-R. Du, Europhys. Lett. 123, 35001 (2018).
- [59] H. Huang, A. V. Ivlev, V. Nosenko, W. Yang, and C.-R. Du, Phys. Rev. E 107, 045205 (2023).
- [60] A. P. Thompson, H. M. Aktulga, R. Berger, D. S. Bolintineanu, W. M. Brown, P. S. Crozier, P. J. in 't Veld, A. Kohlmeyer, S. G. Moore, T. D. Nguyen *et al.*, Comput. Phys. Commun. 271, 108171 (2022).
- [61] L. Couëdel, V. Nosenko, A. V. Ivlev, S. K. Zhdanov, H. M. Thomas, and G. E. Morfill, Phys. Rev. Lett. 104, 195001 (2010).
- [62] A. V. Ivlev and R. Kompaneets, Phys. Rev. E 95, 053202 (2017).
- [63] A. V. Zampetaki, H. Huang, C.-R. Du, H. Löwen, and A. V. Ivlev, Phys. Rev. E 102, 043204 (2020).
- [64] A. Ghosh, V. K. Chikkadi, P. Schall, J. Kurchan, and D. Bonn, Phys. Rev. Lett. 104, 248305 (2010).
- [65] K. Chen, T. Still, S. Schoenholz, K. B. Aptowicz, M. Schindler, A. C. Maggs, A. J. Liu, and A. G. Yodh, Phys. Rev. E 88, 022315 (2013).
- [66] M. L. Falk and J. S. Langer, Phys. Rev. E 57, 7192 (1998).
- [67] Y. M. Beltukov, C. Fusco, A. Tanguy, and D. A. Parshin, J. Phys. Conf. Ser. 661, 012056 (2015).
- [68] H. Mizuno, H. Shiba, and A. Ikeda, Proc. Natl. Acad. Sci. U.S.A. 114, E9767 (2017).
- [69] E. Lerner, G. Düring, and E. Bouchbinder, Phys. Rev. Lett. 117, 035501 (2016).
- [70] G. Kapteijns, E. Bouchbinder, and E. Lerner, Phys. Rev. Lett. 121, 055501 (2018).
- [71] Y.-C. Hu and H. Tanaka, Nat. Phys. 18, 669 (2022).
- [72] L. Wang, G. Szamel, and E. Flenner, Phys. Rev. Lett. 127, 248001 (2021).
- [73] F. Arceri and E. I. Corwin, Phys. Rev. Lett. 124, 238002 (2020).
- [74] Z. Donkó, J. Goree, P. Hartmann, and K. Kutasi, Phys. Rev. Lett. 96, 145003 (2006).
- [75] C. Durniak and D. Samsonov, Phys. Rev. Lett. 106, 175001 (2011).
- [76] P. Schall, D. A. Weitz, and F. Spaepen, Science **318**, 1895 (2007).
- [77] M. J. Falk, V. Alizadehyazdi, H. Jaeger, and A. Murugan, Phys. Rev. Res. 3, 033291 (2021).
- [78] C. Balbuena, M. Mariel Gianetti, and E. Rodolfo Soulé, Soft Matter 17, 3503 (2021).
- [79] H. Tanaka, H. Tong, R. Shi, and J. Russo, Nat. Rev. Phys. 1, 333 (2019).
- [80] R. Dasgupta, H. G. E. Hentschel, and I. Procaccia, Phys. Rev. Lett. 109, 255502 (2012).
- [81] X. Cao, A. Nicolas, D. Trimcev, and A. Rosso, Soft Matter 14, 3640 (2018).

- [82] S. Kang, D. Wang, A. Caron, C. Minnert, K. Durst, C. Kübel, and X. Mu, Adv. Mater. 35, 5498 (2023).
- [83] A. Kumar and I. Procaccia, Europhys. Lett. **145**, 26002 (2024).
- [84] D. Bi, X. Yang, M. C. Marchetti, and M. L. Manning, Phys. Rev. X 6, 021011 (2016).
- [85] S. Lecuyer, R. Stocker, and R. Rusconi, New J. Phys. 17, 030401 (2015).
- [86] Z. You, D. J. G. Pearce, A. Sengupta, and L. Giomi, Phys. Rev. X 8, 031065 (2018).
- [87] S. Dey, A. Bhattacharya, and S. Karmakar, Nat. Commun. **16**, 5498 (2025).
- [88] A. Bottinelli, D. T. J. Sumpter, and J. L. Silverberg, Phys. Rev. Lett. **117**, 228301 (2016).
- [89] A. Bottinelli and J. L. Silverberg, Front. Appl. Math. Stat. 3, 26 (2017).